

N63-15471  
code 1

# TECHNICAL NOTE

## D-1196

A STUDY OF THE EFFECT OF MULTI-G ACCELERATIONS  
ON NUCLEATE-BOILING EBULLITION

By Robert W. Graham and Robert C. Hendricks

Lewis Research Center  
Cleveland, Ohio

NATIONAL AERONAUTICS AND SPACE ADMINISTRATION  
WASHINGTON

May 1963

38P

554365

NATIONAL AERONAUTICS AND SPACE ADMINISTRATION

---

TECHNICAL NOTE D-1196

---

A STUDY OF THE EFFECT OF MULTI-G ACCELERATIONS  
ON NUCLEATE-BOILING EBULLITION

By Robert W. Graham and Robert C. Hendricks

SUMMARY

15471

The effects of multi-g accelerations directed toward a heater surface for near-saturated and subcooled nucleate pool boiling were studied in a centrifuge. High-speed motion pictures and heat-transfer data were obtained in the test program. Subcooling effects were observed to be more significant than the acceleration effects. Acceleration did not appreciably influence the overall heat transfer when the nucleate boiling was characterized by vapor columns or bubble conglomerates. Acceleration did, however, influence the heat transfer in the vicinity of a site for discrete bubbles near the thermal threshold of nucleate boiling. For this case, maximum bubble size, growth rate, frequency, and site activation were influenced by the acceleration magnitude.

INTRODUCTION

In recent years there has been considerable interest in the mechanism of nucleate boiling because boiling-heat-transfer processes often show considerably improved cooling capabilities over single-phase convective processes. One of the more important factors in the nucleate-boiling mechanism is the buoyancy or body-force effect that contributes to the control of the ebullition process.

In applications of boiling heat transfer to missiles or space vehicles, where the body force may range from zero to several g's, the effect of this variance in body-force magnitude and direction must be assessed. References 1 to 3 contain studies of pool boiling of water in centrifuge devices where acceleration forces greater than normal gravity were directed toward the heating element. Both reports investigated the shape of the boiling curve (heat flux as a function of temperature difference) over a range of accelerations. Reference 3 also reports the effects of acceleration on burnout. For the pool and heater geometry studied, the magnitude of the burnout flux is proportional to the one-fourth power of the acceleration when the acceleration force is greater than 10 g's. The scatter in the burnout-heat-flux results was within the limits predicted by reference 4 (pp. 15-46).

Reference 1 shows particular interest in the effect of acceleration on the peak heat flux (maximum heat flux in nucleate regime). The data of reference 1 are compared with the equation of Borishanskii (ref. 5), which was developed to predict the maximum heat flux for nucleate pool boiling. The experimental peak

heat flux did seem to follow the acceleration term  $(a/g)^{0.25}$  where  $a$  is acceleration and  $g$  is gravitational acceleration. Another interesting aspect discussed in reference 1 is the effect of acceleration on the number of nucleation sites. It is concluded that, for a moderate constant heat flux, fewer sites were active as the acceleration was increased. At high heat fluxes, acceleration had little effect on the number of active sites.

The pool-boiling mechanism at zero gravity or near zero gravity was examined experimentally; the results are presented in reference 6. The absence of the buoyancy force at zero gravity arrested the ebullition process, and a filmlike phenomenon was evident. Burnout data taken at small accelerations seemed to follow the one-fourth power of the acceleration. At precisely zero gravity, the burnout flux could not be predicted by this correlation because the correlation would predict that burnout would occur at zero heat flux.

It is evident from the work that has been done that variations in the buoyancy force can produce appreciable effects on the nucleate-boiling heat-transfer results. The purpose of this report is to determine whether the body force has any pronounced effects on the model of the nucleate-boiling mechanism. Such important factors as bubble growth rate, bubble frequency, number of nucleation sites, maximum bubble size, and waiting period will be examined for their dependence upon (or independence of) the magnitude of the body force. These results will serve as a test of the model postulated to describe the nucleate-boiling mechanism.

Included in this report are data for heat rate as a function of temperature difference (surface minus bulk) over a range of accelerations. Some of these data will pertain to a very active boiling surface and some to a surface where only an isolated bubble site is active. The effect of acceleration on these two cases will be discussed. No "burnout" conditions were studied.

The degree of subcooling was varied to evaluate its influence on the boiling curves (heat flux as a function of temperature difference). The relative influence of subcooling and acceleration on the boiling curves is discussed.

Shadowgraph motion-picture photography was used to examine the effect of acceleration on the circulation of the fluid adjacent to the heating strip. Motion-picture supplement C-218 has been prepared and is available on loan. A request card and a description of the film are included at the back of this report.

## APPARATUS

Figure 1(a) shows the 4-foot-arm centrifuge apparatus used to simulate the varying body forces in the fluid. The arm was rotated by an air turbine, and the speed was measured on a tachometer. The high-speed movie camera and the lamp mounted adjacent to the pool boiler were used in photographing the bubbles.

The tank and the heating element are shown in figure 1(b). The tank was approximately 2 quarts in volume and was equipped with observation and illumination windows for the photography. The tank was mounted on a free-rotating trunnion

arrangement that automatically enabled the tank-heater assembly to be oriented so that the resolved acceleration vector (gravity plus centrifugal) was perpendicular to the heater surface. The tank was so constructed that either a partial vacuum or a positive gage pressure could be maintained above the liquid surface. This feature was valuable in establishing the thermodynamic state of the water for various boiling conditions.

The heating element was a thin Chromel ribbon mounted over a bakelite block. The ribbon was tension-mounted with springs on each end and was cemented to the surface of the bakelite block. The purpose of the tension mounting was to prevent buckling of the strip when it expanded during heating. By virtue of this mounting, the ribbon heated the fluid from one side only. The heat flux from this heater was essentially constant over the entire length of the ribbon. For all the experimental runs reported herein, the acceleration vector was directed toward the heater surface in contact with the water. The aforementioned film supplement illustrates how film boiling can be induced by reversing the direction of the acceleration vector.

A portion of the experimental program was devoted to examining the effect of the tank-heater geometry on the boiling process. Two geometries were utilized (figs. 1(c) and (d)). The latter has a transparent shield mounted so as to restrict the circulation patterns of the fluid immediately above the heater ribbon. Results from tank-heater geometry with and without shields are compared.

The heating elements were instrumented with small-gage thermocouples to measure the surface temperature. Thermocouples were also used to monitor the fluid bulk temperature. For most of the runs reported herein, the tank was vented to atmosphere; thus the fluid pressure at the tank vent was assumed to be 1 atmosphere. For those runs in which the tank was run at partial vacuum, a mercury manometer was used to measure the pressure before and after the run. The electrical power applied to the strip configuration was obtained from voltage and current measurements. Voltage-tap leads were soldered to the heating strip to get a more precise measurement of the power dissipated in the strip. All the measurements monitored while the centrifuge was rotating were brought through mercury sliprings and recorded either on an oscillograph or by a digital voltmeter.

## PROCEDURE

In all the tests in which the heating strip was instrumented, the fluid used was distilled, degassed water. In some preliminary runs, ethyl alcohol was used. The procedure of filling the tank with distilled, degassed water was followed carefully to prevent contamination from the air.

Essentially, two types of running procedure were followed in gathering data. One was to run the centrifuge at a given speed (constant acceleration) and then vary the power to the strip; the other was to vary the centrifuge speed while keeping the power constant.

The degree of subcooling was rigidly controlled throughout the experimental procedure by continuously monitoring the bulk temperature. The increased head of

fluid on the heater ribbon at high multi-g's was compensated for by increasing the bulk temperature so that surface boiling occurred at a subcooling that was comparable to the 1-g case. Cartridge heaters within the tank were used to control the bulk temperature. These heaters were always off during a data run.

Most of the data was obtained within the heat-flux range of 0 to 0.27 Btu per square inch per second. The acceleration was varied from 1 to 10 g's, and the pressure was maintained at 1 atmosphere. A limited amount of data was gathered at a partial vacuum (3 cm Hg abs). For the test conditions at 1 atmosphere, the bulk temperature was set at approximately 200° and 180° F, respectively, in order to assess the subcooling effects. At the partial vacuum condition, the fluid temperature was maintained around room temperature for near-saturation conditions.

## RESULTS AND DISCUSSION

In this experimental program heat flux, acceleration, bulk temperature (or degree of subcooling), and heater geometry were varied independently. For the convenience of the reader, the principal effects observed will be sorted out and related to one or more of these parameters in the following discussion.

### Effect of Subcooling

The boiling-heat-transfer literature states that the degree of subcooling greatly influences the nucleate-boiling curve (heat flux as a function of temperature difference). For example, figure 2 shows a family of boiling curves obtained from one of the heater ribbons used in this investigation. It is apparent from this figure that only a small change in the subcooling (about 30° F max.) produced appreciable changes in the boiling curves. Consequently, great care was exercised to control the degree of subcooling within a narrow tolerance throughout the experimental program. Without such care it might be difficult to discern whether changes in the boiling curves were attributable to acceleration or subcooling effects.

Also shown in figure 2 is a "hysteresis" curve that illustrates the sensitivity of the boiling curves to the manner in which they are developed experimentally. The arrows indicate the "path" taken in obtaining the curves. It is obvious that the two curves are different depending on whether the mode of operation is from low-heat rate to high-heat rate or vice versa. Evidently the history of the thermal layer affects the boiling process. This history can be changed by the experimental manner of approach to a given point on the boiling curve.

While this hysteresis phenomenon is not adequately understood, it is postulated that the thermal sublayer is sensitive to the heating history. High-speed schlieren photographs of the thermal layer (ref. 7) illustrate the dynamic nature of the thermal layer before and after a bubble ebullition event. These pictures indicate that the heating history influences the growth rate and thermal state of the sublayer. In reference 8, the nature of the sublayer is shown to be influential in determining site activation.

All of the boiling curves of figures 2 to 6, with the exception of the hysteresis curve in figure 2, have been developed by allowing the heat flux to increase progressively.

### Effect of Acceleration on Boiling (Active Surface)

The principal object of the research program discussed herein was to ascertain if acceleration (body force) had a marked effect on nucleate pool boiling. It was observed in a preliminary study that the orientation of the acceleration vector (toward or away from the heater surface) had a marked effect on the boiling. By directing the vector away from the heater, film boiling conditions would occur at a heat flux generally associated with nucleate boiling when ordinary gravity was directed toward the heater.

Figure 3 is a plot of heat flux as a function of the difference between surface and bulk temperatures for a range of accelerations. This surface temperature represents the readings of one thermocouple at a section of a heater where several sites were very active. (High-speed motion pictures showed considerable boiling activity.) The bulk temperature was carefully controlled to produce the same amount of subcooling over the entire range of acceleration values. Figure 3 shows that increased acceleration did tend to translate the boiling curve upward to higher heat flux for a given temperature difference. This translation is attributed to enhanced natural convection heat transfer over the nonboiling areas of the heater. More will be said about natural convection in discussing figures 5, 6, and 12.

The boiling curves in figure 3 all show the same general trends in curvature. As was mentioned earlier, there were many active sites in this section of the heater. Also, for the greater portion of the boiling curves the boiling mechanism was well advanced beyond incipient boiling to a condition where vapor columns were prevalent. High-speed photography showed that these vapor columns were active over the entire range of accelerations investigated. Consequently, the variation in acceleration had little effect on this type of boiling mechanism, which explains the general similarity of the boiling curves over a range of accelerations.

### Comparison of Subcooling and Acceleration Effects

It is also interesting to compare the relative effects of acceleration and subcooling on boiling, which is characterized by vapor columns and bubble conglomerates. Figure 4 shows data for this type of boiling taken at 12° and 32° subcooling for both 3 and 9 g's of acceleration. It is very clear from these curves that the subcooling effects are pronounced, whereas the acceleration effects are almost negligible. This figure provides further verification that acceleration does not greatly affect the boiling mechanism for heat-flux conditions well beyond the incipient boiling threshold.

## Effect of Acceleration on Incipient Boiling

The observation made concerning the small effect of acceleration pertains to a particular regime of the boiling mechanism (vapor columns); it does not necessarily apply to the upper limit of nucleate boiling, which was not investigated herein, or to the incipient point where a discrete number of sites are just becoming active. The latter situation was also observed in these experiments. Figure 5 contains boiling curves obtained from a different segment of the same heater strip. For some reason (probably surface conditions), this segment was comparatively dormant. The 1-g curve (fig. 5) shows that a boiling phenomenon began at a temperature difference of  $46.5^{\circ}$ . Up to that point heat was transferred by free convection only. For 3 g's of acceleration, the site did not become active, and the free-convection mode continued beyond the temperature difference and heat flux where boiling began for the 1-g case. In references 7 and 8, it is postulated that the incipient conditions for boiling require the development of a thermal layer of definite thickness and thermal condition such that heat can be transferred into the bubble nucleus. Reference 8 presents data that confirm this hypothesis and theory.

Perhaps the increased natural circulation of the fluid at a greater acceleration thinned the thermal sublayer, and thus it could not support a nucleus. Consequently, a natural convection phenomenon persisted to higher values of temperature difference. This subject will be more thoroughly discussed in the section "Site Activation." It is interesting to observe that the level of the natural convection curve for 3 g's is above the 1-g curve (fig. 5). This would be expected as prescribed by a parameter like the Grashof number. In fact, natural-convection correlations, which stipulate that the Grashof number should be raised to the 0.25 power, predict an increase in heat transfer of approximately 30 percent in going from 1 to 3 g's, which is approximately what figure 5 shows. It is interesting to observe that the burnout studies in references 1 and 3 showed the same dependence on acceleration.

It was pointed out in the section entitled "Effect of Acceleration on Boiling (Active Surface)" that acceleration did tend to translate the boiling curve (see fig. 3), upward to higher heat flux for a given temperature difference. This was attributed to a natural-convection component since the entire heating surface is not experiencing ebullition at one time, even in very active boiling. It is speculated that this natural-convection component is significant near the burnout condition. Consequently, the enhanced burnout heat flux induced by multi-g accelerations may be attributed to a natural-convection component. The burnout results of references 1 and 3 indicate that the burnout flux is dependent on  $(a/g)^{0.25}$ , which is the same natural-convection dependence on acceleration noted herein.

## Effect of Shield Geometry

As was mentioned the APPARATUS section, the geometry of the heater-tank assembly was altered by the insertion of a shield above the heater block. Comparison of the heat-transfer data for the shielded and unshielded conditions did show that this geometry change influenced the experimental results. Figure 6 contains these comparative data over a range of acceleration. It is apparent

that the heat-flux values for a given temperature difference are higher for the unshielded geometry than the shielded. Perhaps the "chimney" effect imposed by the shields depresses the boiling mechanism, and natural convection becomes a more significant contributor to the overall mechanism. Certainly the slope of the shielded curve in figure 6 is more similar to that of the free-convection curves (fig. 5) than that of the unshielded curve. The steeper slope of the unshielded geometry indicates a greater contribution by a boiling mechanism.

Figure 6 can be interpreted as further evidence that natural convection is a determining factor in establishing the level of the boiling curves for any heater geometry (fig. 3). A heating surface that is producing a boiling phenomenon may be thought of as comprising areas where ebullition controls the heat transfer (the vicinity of active sites) and other areas where natural convection controls the heat transfer. The average heat-transfer coefficient is an integrated average of these two kinds of areas.

Also of interest in figure 6 is the similar spread of the data for both geometries, which is attributed to acceleration effects. Consequently, in assessing the acceleration effects on the boiling curves, it does not matter which geometry is employed.

### Bubble Growth

Figure 7 contains families of bubble-growth curves for constant heat flux and subcooling with acceleration as a parameter. All of the bubbles emanated from one site on the heating strip. During the growth process on the heater ribbon, the bubbles were oblate spheroids. The principal axial dimensions were measured, and the volume of the oblate spheroid bubbles was computed as a function of time. The radius of a perfect spheroid that would displace the same volume was computed for each increment of time. This radius is the ordinate of figure 7.

The statistical nature of the growth curves is to be expected. As discussed in reference 8, the ebullition process is sensitive to the random nature of the thermal layer adjacent to the heating surface, and this reflects in the bubble growth.

The data shown in figure 7 do show that there is a definite trend for the maximum bubble size and growth rate to diminish as the acceleration is increased. The initial growth rates seem similar, but at later times the bubbles grow slower when the acceleration is greater. Perhaps the enhanced natural circulation of the fluid surrounding a bubble at greater accelerations tends to draw heat away, actually condenses some of the vapor, and thus inhibits growth. The effect of the circulation on the thickness of the thermal layer is discussed in the section "Site Activation."

A portion of the film supplement to this report is devoted to shadowgraph movies of the fluid above the heating strip. The circulation of the fluid above the strip is apparent. As would be expected, the 10-g case exhibits a more pronounced circulation pattern. This is obvious in the films despite the fact that the 10-g case was photographed at twice the film speed of the 1-g case.



## Maximum Bubble Size

The following expression for the maximum bubble size was developed in reference 9:

$$\sqrt[3]{V_b} = 0.0119 \beta \sqrt{\frac{2\sigma}{a(\rho_l - \rho_g)}} \quad (1)$$

where 0.0119 is an empirical constant and

$V_b$  volume of bubble

$\beta$  contact angle of bubble, deg

$\sigma$  surface tension

$a$  local acceleration, ft/sec<sup>2</sup>

$\rho_l$  density of liquid (saturation)

$\rho_g$  density of gas (saturation)

This equation was developed by assuming that the maximum size of the bubble would coincide with the lift-off of the bubble from the surface. The lift-off would occur when the buoyancy force overcomes the surface tension force that retains the bubble at the surface.

The experimental bubble-size data at lift-off were compared with the predictions from the Fritz equation. These comparisons are listed in the following table. Also tabulated are the exponential values of the acceleration required to convert the experimental bubble radius from the 1-g case to the experimental bubble radii of multi-g cases.

Pressure, atm	Acceleration, g's	Maximum experimental radius, in.	Maximum radius from Fritz equation, in.	Exponent on a/g relation
1	1	0.05 - 0.07	0.018	
	7	0.02	.007	-0.56

Two interesting observations can be made from this table. First, for the fluid state established in the tank, the Fritz equation as defined in reference 9 does not predict the maximum size; the experimental bubble radii are greater than the prediction. The Fritz equation (ref. 9) is a correlation of bubble data obtained with water and gaseous-hydrogen bubbles formed in highly diluted solutions; presumably these data were obtained at 1 atmosphere. The experimental maximum bubble radii were taken from figure 7, and these represent bubbles grown in a 1-atmosphere environment. An even poorer agreement with the Fritz equation was observed for the tests made at vacuum conditions (3 cm Hg abs). The experi-

mental bubbles were much larger than those observed at 1 atmosphere. On a heater ribbon, which was not the same as the one used to develop figure 7, the maximum experimental bubble radius at this low pressure was 0.38 inch. The fact that two different heater ribbons were used eliminates any possible comparison of the bubble-size data at the two pressure levels because of the differences in the site sizes.

Even though the absolute magnitudes of the bubble radii as predicted by the Fritz equation do not match the experimental values, the changes in bubble size with gravity do follow the trend predicted by the Fritz relation. The Fritz equation predicts that the bubble size diminishes with the inverse square root of the gravity. This is approximately the value of the exponent derived from the experimental results. It should be noted that the experimental results cover a limited range of gravities (from 1 to 7 g's). Experimental information at greater accelerations is needed before a generalized conclusion on the gravity effect can be finalized.

This apparent disagreement between the experimental bubble radius and the Fritz equation predictions does raise certain questions concerning the ebullition model underlying the equation. Fritz's model assumes a static balance between the buoyancy force and surface tension. High-speed motion pictures of growing bubbles, such as those presented in the film supplement to this report, show very clearly that the circumstances surrounding the lift-off of a bubble are very dynamic. Consequently, some inertia effects have been omitted from the Fritz model. Figure 8 is a schematic representation of the forces present at bubble lift-off. It is easier to enumerate these forces than it is to weight them quantitatively. The force balance  $\vec{F}$  on the bubble can be expressed symbolically in the following manner:

$$\sum \vec{F}_{\text{hydrostatic}} + \sum \vec{F}_{\text{surface tension}} + \sum \vec{F}_{\text{inertia}} = 0 \quad (2)$$

The hydrostatic force is the summation of the static pressure acting externally on the surface of the bubble. It is conceivable that this summation of forces may in some situation actually act to hold the bubble against the surface and may not be a buoyancy force at all. The geometry of the bubble (size of the neck with respect to the bubble volume) or the direction of the acceleration vector will determine whether this summation is a buoyancy or a restraining effect. The latter effect is illustrated in the movie supplement with the film boiling of ethanol in an inverted gravity orientation.

The surface interfacial forces always restrain the bubble from leaving the heating surface. Involved in the interfacial-force terms must be the surface tension, the surface condition, and wettability of the surface. The latter term is implied in Fritz's equation because of the inclusion of contact angle  $\beta$ .

The first two terms of equation (2) are included in a general fashion in Fritz's equation. The third summation, the inertia forces, is not included. Two inertia effects are considered important. Rapid growth of the bubble (see fig. 8) sets into motion a mass of liquid above the bubble that tends to entrain the bubble in its wake. Still another inertia effect is the motion of a mass of

liquid (downwash) that sweeps around the base of the bubble when the neck is being generated. Thus, there is a tendency for the bubble base to experience an upward thrust from the inertia of this field. Some experimental verification of this downwash was observed by the authors of reference 7 when they made high-speed shadowgraph pictures of boiling. Another limitation to the Fritz equation is the fact that it does not include surface effects.

Reference 7 contains a bubble-growth analysis that links bubble size to a characteristic dimension of a site. Such a theory does account for the spectrum of bubble sizes found emanating from a commercial surface.

#### Site Activation

During the course of the experimentation, several heater ribbons were used. Each ribbon had different surface conditions and thus produced different site locations. With a given heater ribbon, as many as 15 sites were active at one time or another, but at no time were all sites active at once.

It was noted that, when the heat flux was increased for a given acceleration, the number of active sites increased. The following tables illustrate this tendency for an absolute pressure of 3 centimeters mercury with a heater ribbon that had a total of nine sites:

Heat flux, Btu (sq in.)(sec)	Active sites
Ordinary gravity	
0.035	1
.086	3
Acceleration, 3 g's	
0.025	0
.08	2
.20	4
.27	5

It has been shown analytically that a greater spectrum of site sizes becomes effective at the higher heat fluxes (ref. 8).

Also of interest is the effect of acceleration on the number of active sites. It has been mentioned previously in connection with figure 5 that an active site can be killed by increasing the acceleration. In fact, at a very moderate constant flux (0.023 Btu/(sq in.)(sec)), where boiling is first evident at several sites along the heater, the number of sites diminished as the acceleration increased. For instance, with a particular shielded heater geometry the total number of sites for a heat flux of 0.023 Btu/(sq in.)(sec) changed in the following manner:

Acceleration, g's	Active sites
1	13
3	7
9	4

Reference 8 has been mentioned several times throughout this report. It contains an analysis and experimental verification, which indicate that there is a relation between cavity size and minimum heat flux for constant heat flux boiling along a heating surface. For the convenience of the reader and to facilitate discussion, the model of bubble instigation, which is basic to the analysis of reference 8, is presented in figure 9. The history of the thermal layer and the bubble nucleus is presented schematically. In figure 9(a) the thermal layer has zero thickness, and consequently no thermal profile is developed. The condition for the instigation of bubble growth is represented by the circle in the temperature-profile plot. In figure 9(b) the thermal layer is developing, and the thermal profile is evident. The profile has not thickened sufficiently to satisfy the thermodynamic condition for bubble growth. In figure 9(c) the boundary layer has grown sufficiently to satisfy the thermodynamic condition for bubble growth. This marks the end of the waiting period. Note that, in the sketches of the temperature profile, the thermal-layer thickness is approximated by a linear temperature distribution. Reference to this approximation is made in the section "Effect of Acceleration on Waiting Period."

In reference 8, the thickness of the laminar thermal layer is assumed to be 3000 microinches. This is the approximate value that was determined experimentally in reference 10. Using this thickness and assuming that heat is transferred through the thermal layer by molecular transport (conduction) only, the author of reference 8 computed the minimum- and maximum-size cavity radius that would bear a bubble at a given heat flux.

If it is assumed that increasing the acceleration thins the laminar-thermal-layer thickness, the curve that establishes the minimum flux to cause a site to be active would depend upon the acceleration level. Such a family of curves is presented in figure 10. As was mentioned in discussing figure 5, the natural convective heat transfer (no boiling) was enhanced by increasing the acceleration; it was also pointed out that the increase in heat transfer seemed to follow a conventional Grashof correlation in which the exponent on the Grashof number is 0.25. Starting with a value of 3000 microinches for ordinary gravity, the laminar layer thickness was diminished inversely with the Grashof number raised to the 0.25 power in computing the curves shown in figure 10.

Superposed on figure 10 are actual data points obtained from a heater ribbon that had an obvious surface scratch approximately 0.001 inch wide. Figure 11 is a magnified picture of this site. Fortunately, this was an isolated site and it was near one of the surface thermocouples so that the effect of ebullition on surface temperature was apparent. Figure 12 is a family of boiling curves in which the surface temperature data were obtained from the aforementioned thermocouple. The approximate point where boiling begins for each curve is marked by

a solid symbol. The heat fluxes for incipient boiling from figure 12 and the measured size of the site scratch comprise the data used in the labeled points in figure 10. It is interesting to observe that these data points all fall to the right of the respective curves marking the minimum threshold of heat flux (fig. 10) for each acceleration.

From figure 10 it is therefore concluded that increased acceleration thins the laminar layer and thus promotes a higher threshold of heat flux before a bubble can be conceived at a given site.

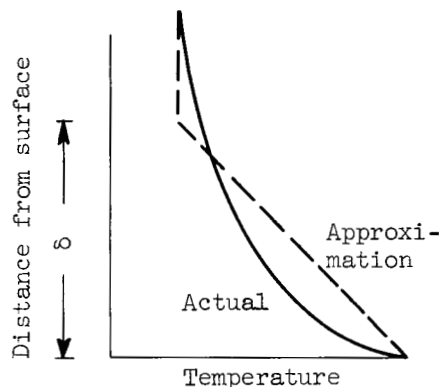
#### Effect of Acceleration on Waiting Period

In reference 7 the waiting period is defined as the time interval beginning with the separation of a bubble from the surface and ending where a new bubble appears (see fig. 9). When a bubble leaves a site, the thermal boundary layer in that vicinity is partially destroyed. The waiting period represents the time required for the thermal layer to reestablish itself. The period of a bubble comprises the waiting period and the bubble-growth period. As is pointed out in reference 7, the waiting period may be greater than, equal to, or less than the growth period. In any case, the waiting period or the ratio of the waiting period to the growth period is important in describing the bubble ebullition process and the attendant heat transfer.

The high-speed movies show that the ratio of the waiting period to growth period at a given site increases with magnitude of the acceleration. For instance, at ordinary gravity the ratio of the waiting period to the growth period for three successive bubbles at a site was 2.06, 5.8, and 2.06 at the same site, but at 7 g's this ratio went to 10 for two successive bubbles.

This trend is explainable in terms of the model for bubble growth presented in reference 7. The trend is also consistent with the deactivation of sites observed when the acceleration is increased (fig. 5). When a site is deactivated, the waiting period goes to infinity.

The bubble-growth model presented in reference 7 stipulated that the thermal layer could be approximated by a linearized temperature profile. As is pictured in the following sketch, the thermal layer is divided into two regions. Over a



thickness  $\delta$ , the heat transport mechanism is assumed to be conduction only. Beyond this  $\delta$ , eddy diffusion controls the heat-transfer mechanism, and the fluid temperature is constant and equal to the bulk temperature. The eddy diffusion in this region is controlled by the tank and heater geometry as well as the acceleration magnitude. At high accelerations, the eddy diffusivity is enhanced, which results in a thinning of the laminar sublayer  $\delta$ . As is shown in figure 10, thinning of the thermal layer increases the heat-flux threshold necessary for ebullition. If a transient conduction mechanism is assumed in the laminar thermal layer, a longer time period will be required to satisfy the thermodynamic state at some distance  $x_b$  away from the surface (see fig. 9) before a nucleus will grow into a bubble. This is the same as saying the waiting period will be longer.

#### CONCLUDING REMARKS

The degree of subcooling is more influential in controlling the pool-boiling heat flux than is acceleration. Increasing the acceleration, when directed toward the heater surface, (1) does improve the natural-convection component of heat transfer that is present with nucleate boiling, (2) delays the incipience of bubbles at a site to a higher heat-flux threshold, and (3) reduces the maximum size, growth rate, and frequency of discrete bubbles emanating from a site. Directing the acceleration vector away from the heater leads to film boiling at modest heat fluxes.

#### SUMMARY OF RESULTS

Over the range of accelerations, liquid states, and heater geometries employed in these tests, the following observations concerning the boiling process in a multi-g environment can be stated:

1. Acceleration when directed toward the heater geometry does increase the heat-flux threshold necessary for the incipience of boiling at a site. Acceleration, however, has little effect on the boiling mechanism at high heat fluxes well beyond the threshold of incipience where vapor columns rather than discrete bubbles are evident. This observation is in agreement with the results obtained by Merte and Clark.

2. It was observed that subcooling had a pronounced effect on the nature of the boiling curve. Even small changes on the order of  $2^\circ\text{F}$  produced significant changes; thus, subcooling appears to be a more significant parameter than acceleration in determining the heat transfer associated with boiling.

3. Near the incipient boiling condition, increasing the acceleration decreases the number of active sites. This trend was consistent with the theory that predicts that some sites would "die" if the acceleration was increased.

4. Increasing the acceleration did improve natural convection. This was evident in both the nonboiling and boiling conditions. In the boiling regime, some of the surface is transferring heat by natural convection as well as by the boiling mechanism; thus the total heat transfer consists of boiling and convective contributions. For nonboiling conditions, changes in acceleration produced

increases in heat transfer as predicted by Grashof number raised to the 0.25 power. Perhaps the enhanced burnout flux at multi-g accelerations is attributable to the improved natural-convection component of heat transfer.

5. The geometry of the heater tank does influence the heat transfer. When the heater ribbon was surrounded by a chimneylike shield, the heat flux for a given temperature difference was less than when no shielding was present. This is further evidence of the significance of free convection on the overall heat transport.

6. The growth rate and maximum bubble size are diminished by increasing the acceleration.

7. For ebullition there is a trend for the ratio of the waiting period to the growth period to increase with acceleration. The situation when a site becomes inactive can also be labeled as the occurrence of infinite waiting period; thus, it can be reasoned that the effect of acceleration drives the waiting period toward infinity. Such observation is consistent with the boiling model presented in NASA TN D-594.

Lewis Research Center

National Aeronautics and Space Administration

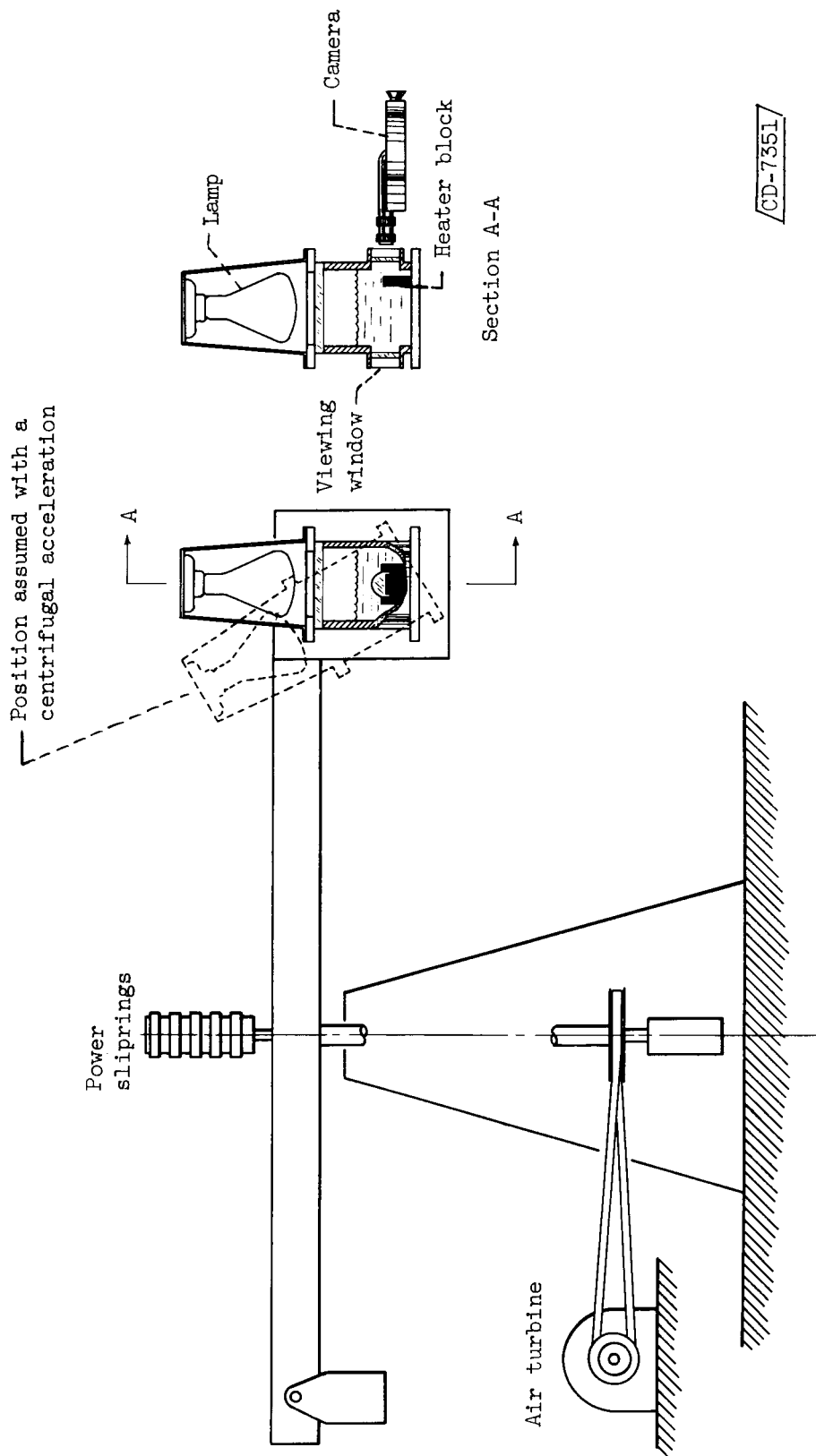
Cleveland, Ohio, January 2, 1963

#### REFERENCES

1. Merte, H., Jr., and Clark, J. A.: A Study of Pool Boiling in an Accelerating System. Tech. Rep. 3, College Eng., Univ. Mich., Nov. 1959.
2. Costello, Charles P., and Tuthill, William E.: Effects of Acceleration on Nucleate Pool Boiling. Mech. Eng. Dept., Univ. Wash., 1960.
3. Costello, C. P., and Adams, J. M.: Burnout Heat Fluxes in Pool Boiling at High Accelerations. Mech. Eng. Dept., Univ. Wash., 1960.
4. Zuber, N., and Tribus, M.: Further Remarks on the Stability of Boiling Heat Transfer. AECU 3631, AEC, Jan. 1958.
5. Borishanskii, V. M.: An Equation Generalizing Experimental Data on the Cessation of Bubble Boiling in a Large Volume of Liquid. Soviet Phys.-Tech. Phys., vol. 1, no. 2, 1956, pp. 438-442.
6. Usiskin, C. M., and Siegel, R.: An Experimental Study of Boiling in Reduced and Zero Gravity Fields. Paper 60-HT-10, ASME-AIChE, 1960.
7. Hsu, Yih-Yun, and Graham, Robert W.: An Analytical and Experimental Study of the Thermal Boundary Layer and Ebullition Cycle in Nucleate Boiling. NASA TN D-594, 1961.

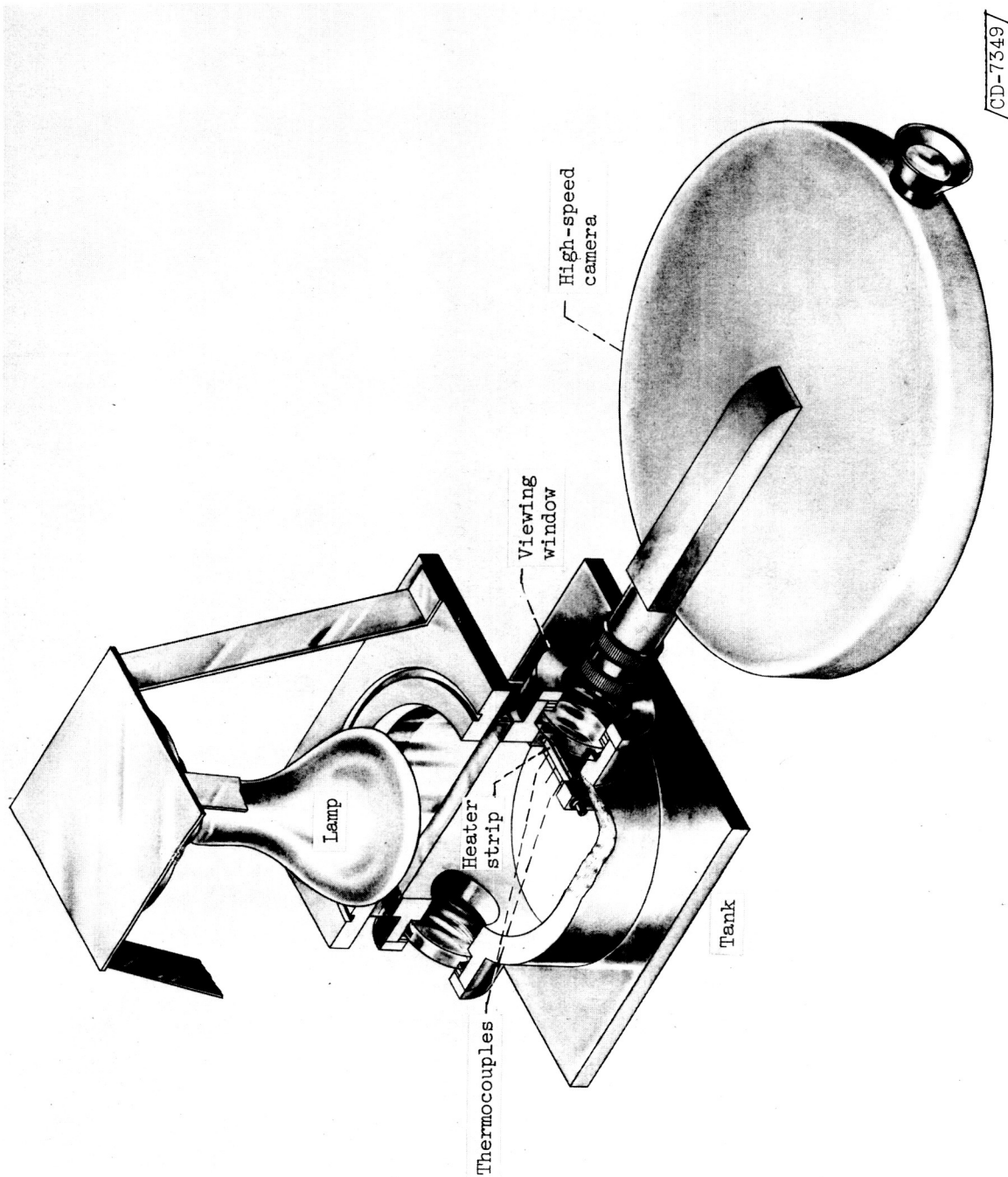
8. Hsu, Y. Y.: On the Size Range of Active Nucleation Cavities on a Heating Surface. Jour. Heat Transfer, ser. C, vol. 84, no. 3, Aug. 1962, pp. 207-213; discussion, pp. 213-216.
9. Jakob, Max: Heat Transfer. Vol. I. John Wiley & Sons, Inc., 1949, pp. 630-631.
10. Treshchev, G. G.: Experimental Investigation of the Mechanism of Heat Transfer in Surface Boiling. Teploenergetika, vol. 4, no. 5, 1957, pp. 44-48.



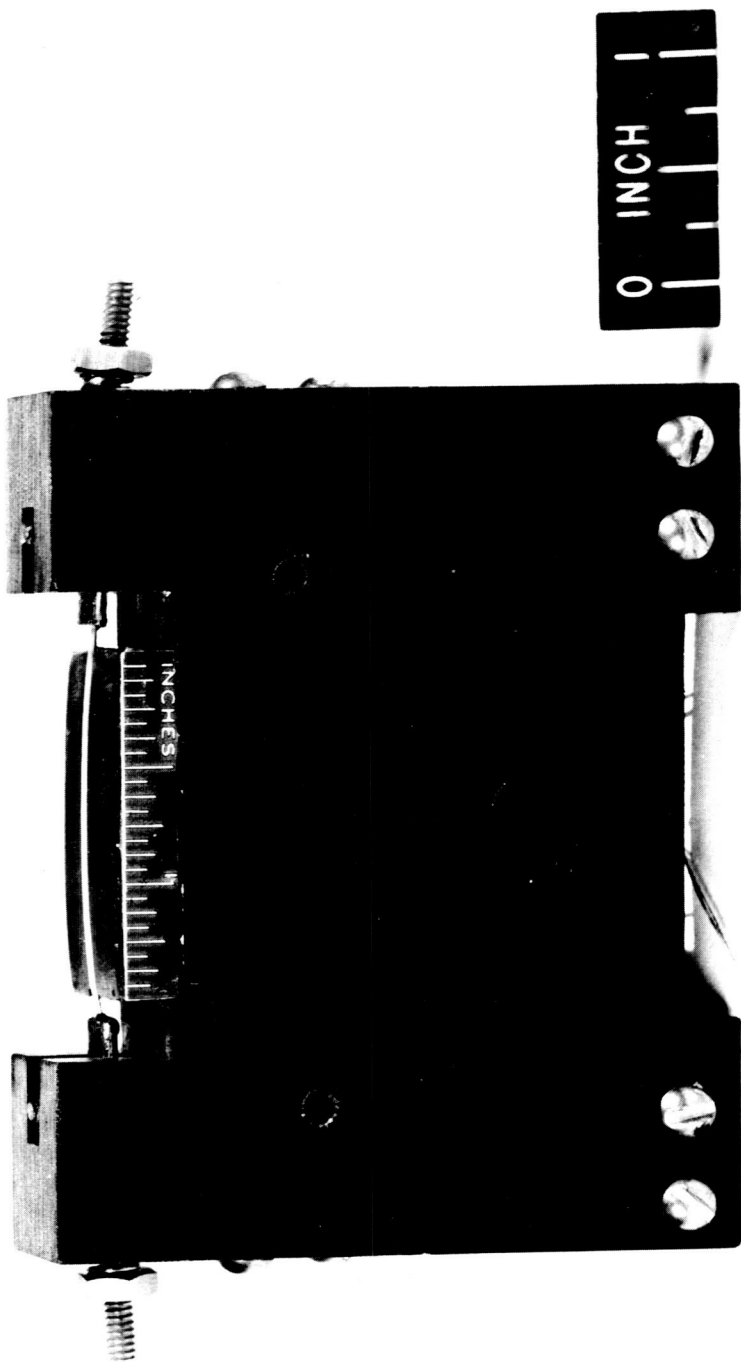


(a) Centrifuge assembly.

Figure 1. - Centrifuge apparatus.



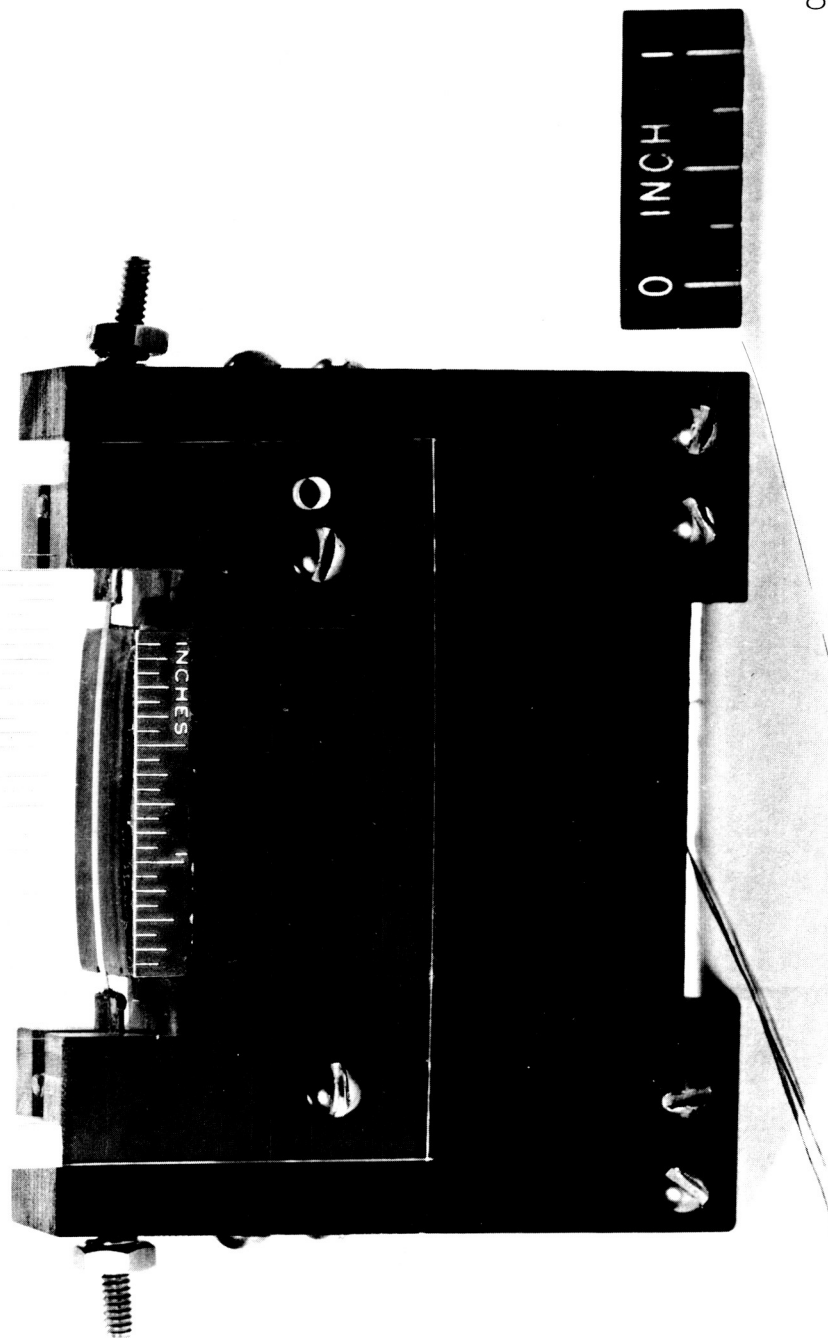
(b) Tank and camera assembly.  
Figure 1. - Continued. Centrifuge apparatus.



C-61743

(c) Heater geometry without shields.

Figure 1. - Continued. Centrifuge apparatus.



C-61742

(d) Heater geometry with shields.

Figure 1. - Concluded. Centrifuge apparatus.

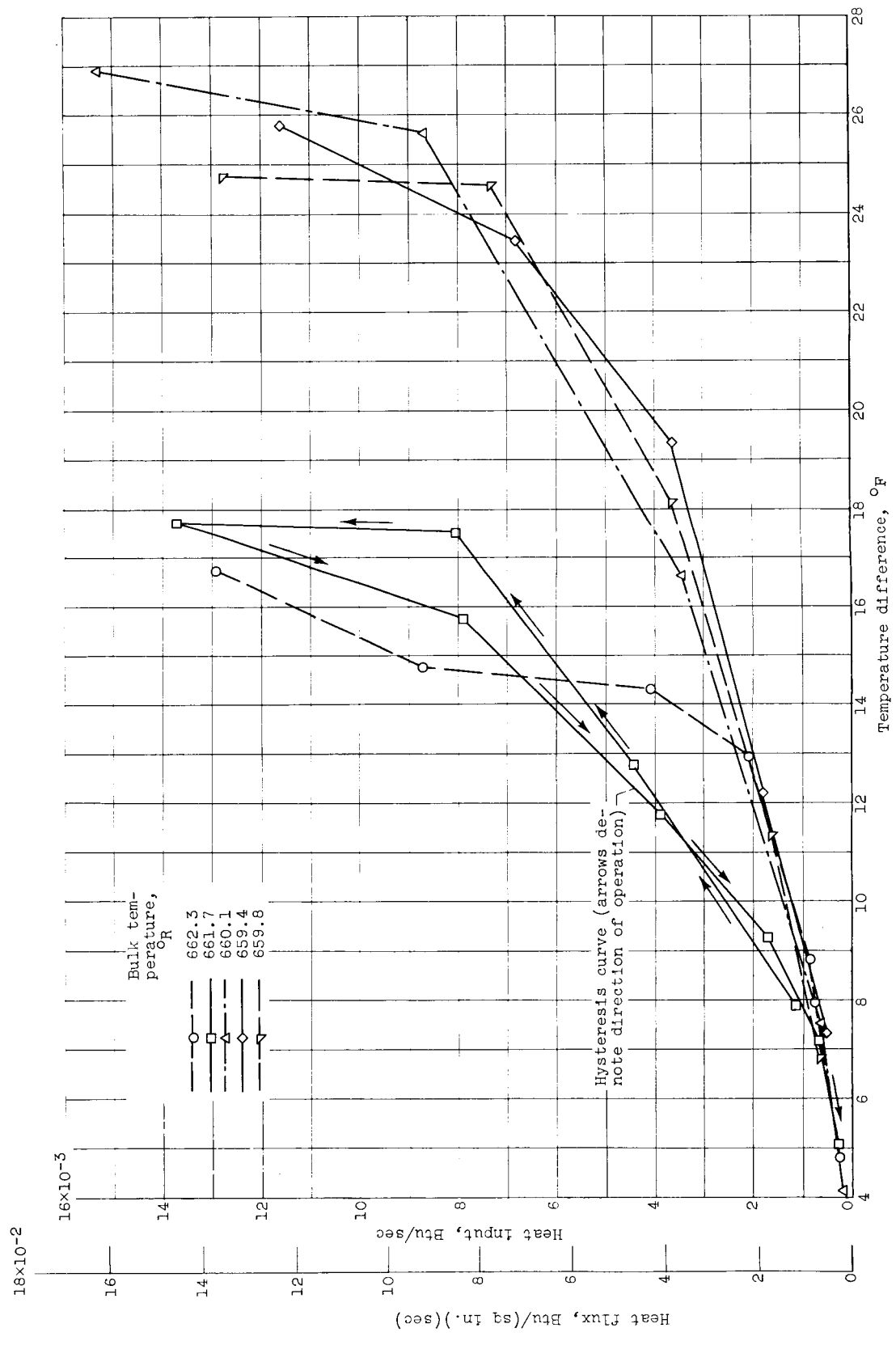


Figure 2. - Influence of subcooling on boiling curves in ordinary gravity. Heater geometry with shields. Water, 1 atmosphere.

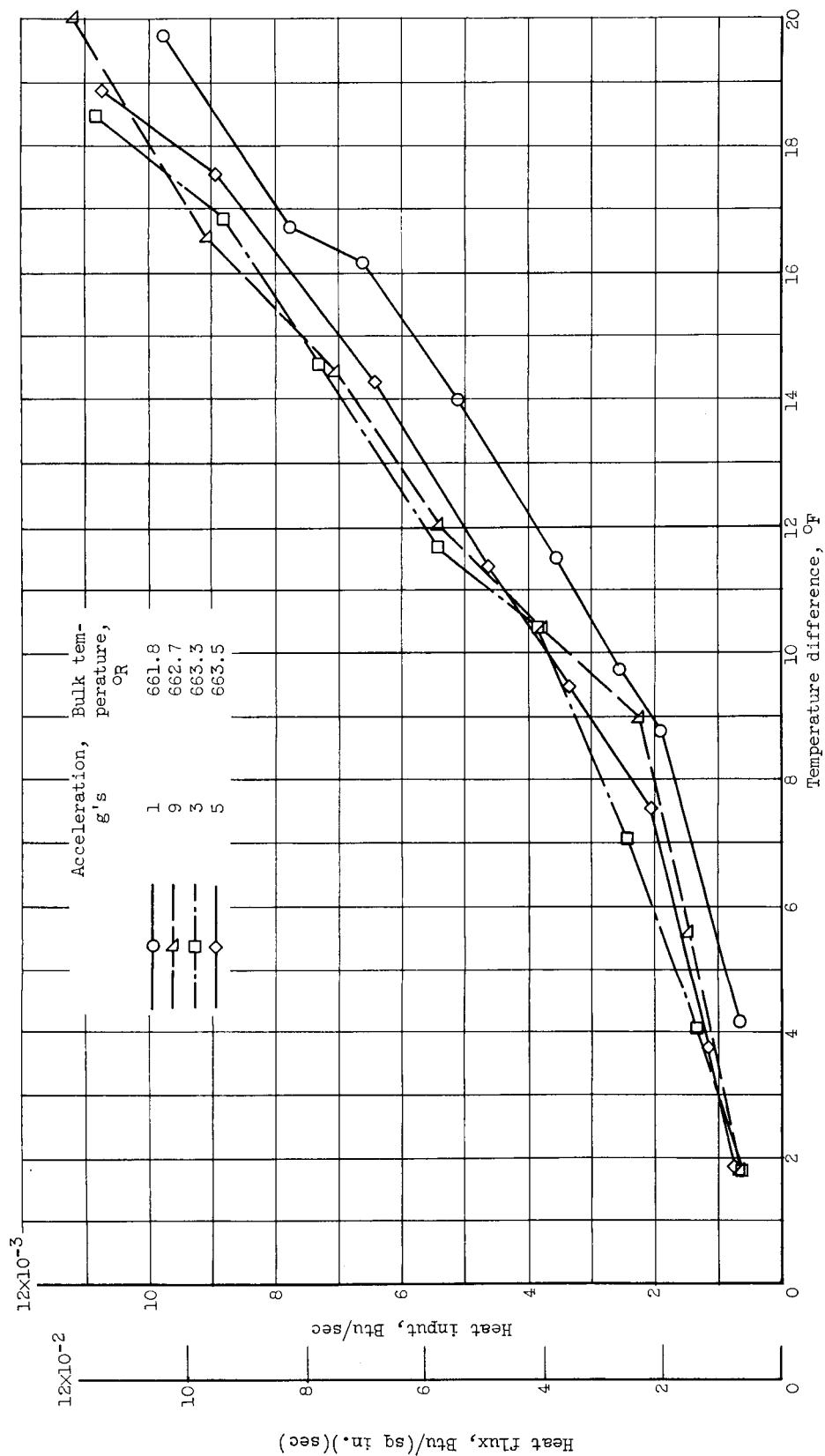


Figure 3. - Pool-boiling heat flux as a function of surface and bulk temperature for a range of accelerations (active segment of heater ribbon). Heater geometry without shields; bulk temperature, ~200° F; water, 1 atmosphere.

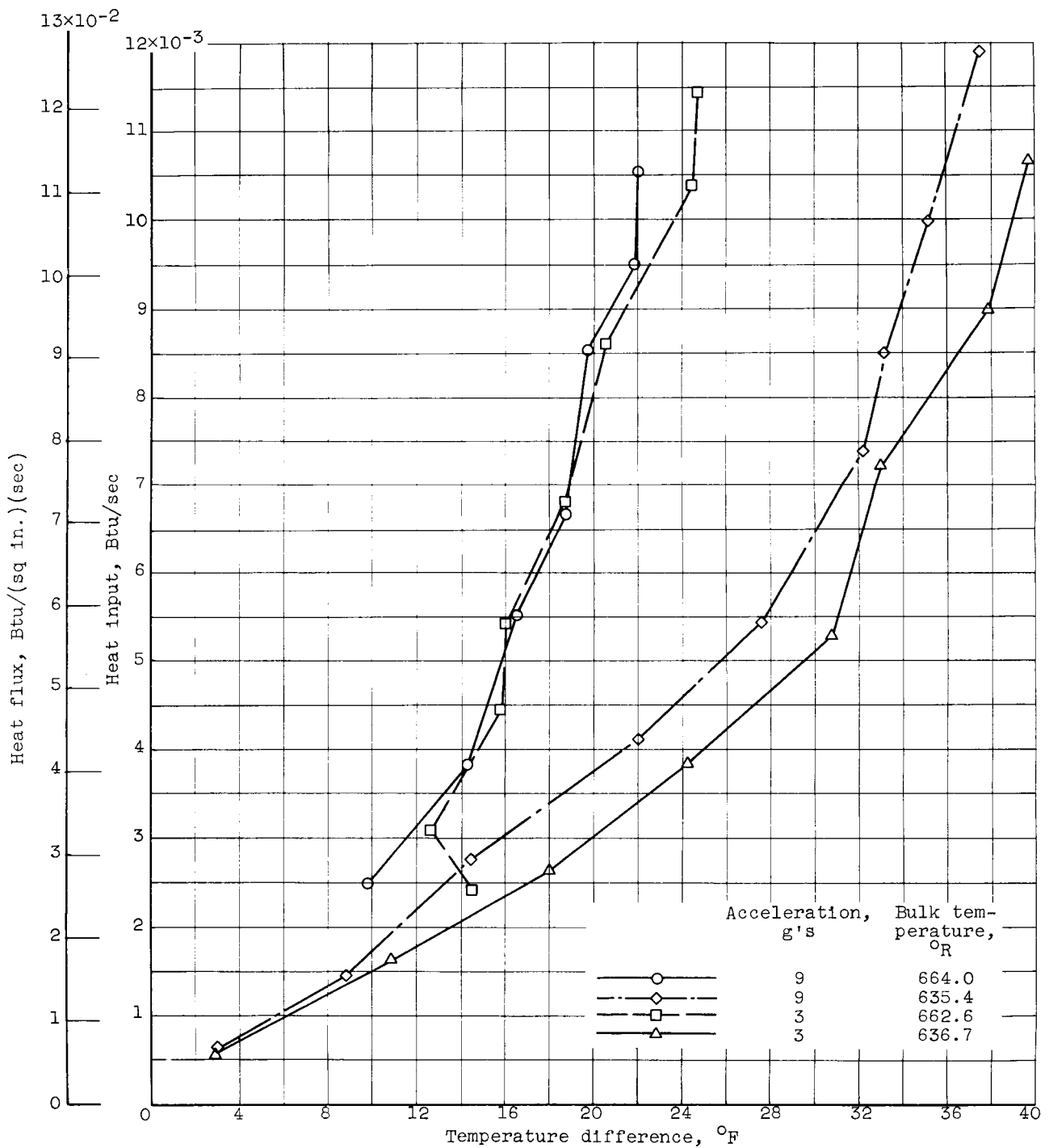


Figure 4. - Influence of subcooling on boiling curves in multi-gravity accelerations. Heater geometry with shields; water, 1 atmosphere.

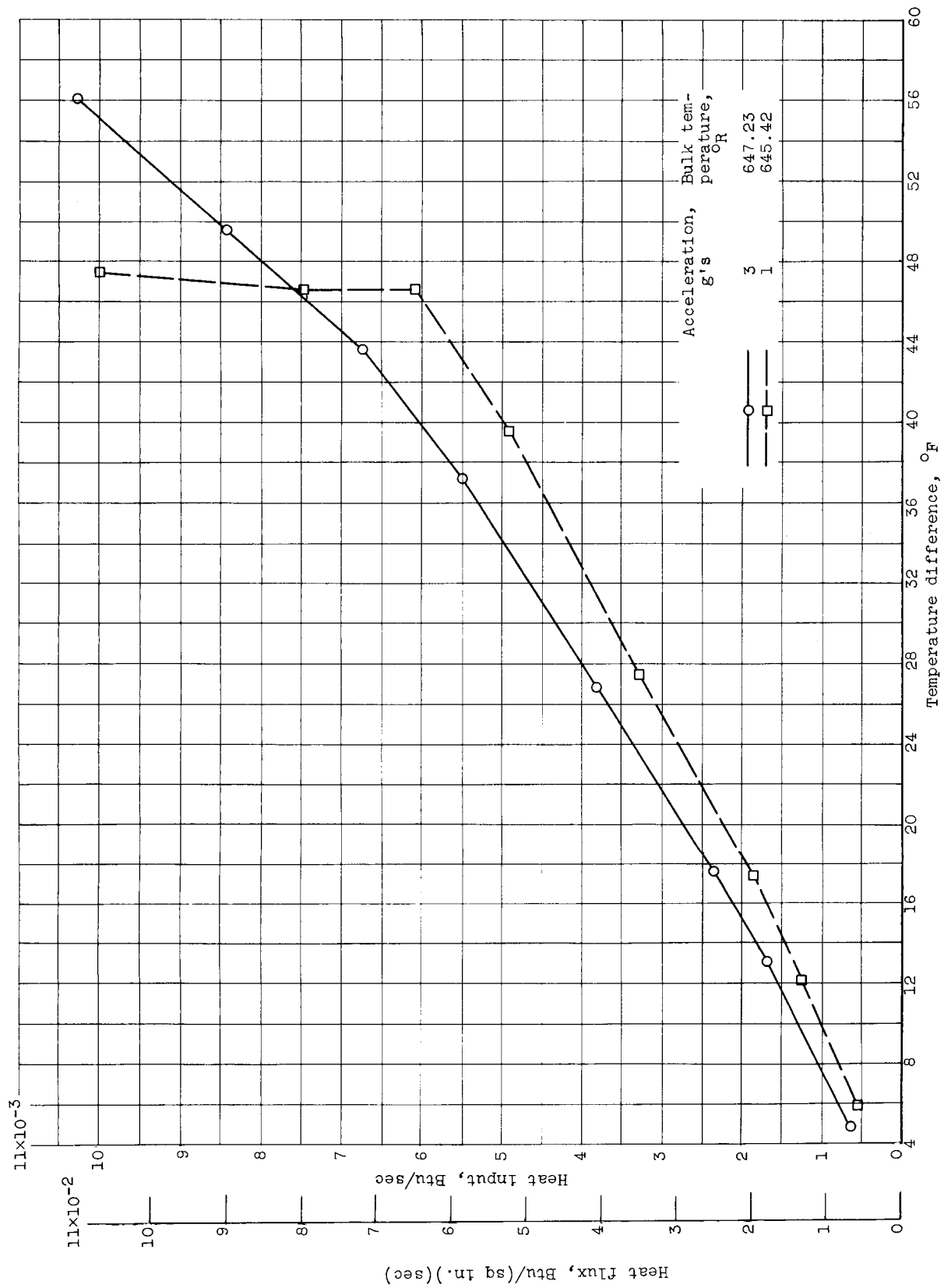


Figure 5. - Effect of acceleration on incipient threshold of nucleate boiling (inactive segment of heater ribbon). Heater geometry without shields; bulk temperature, ~180° F; water, 1 atmosphere.



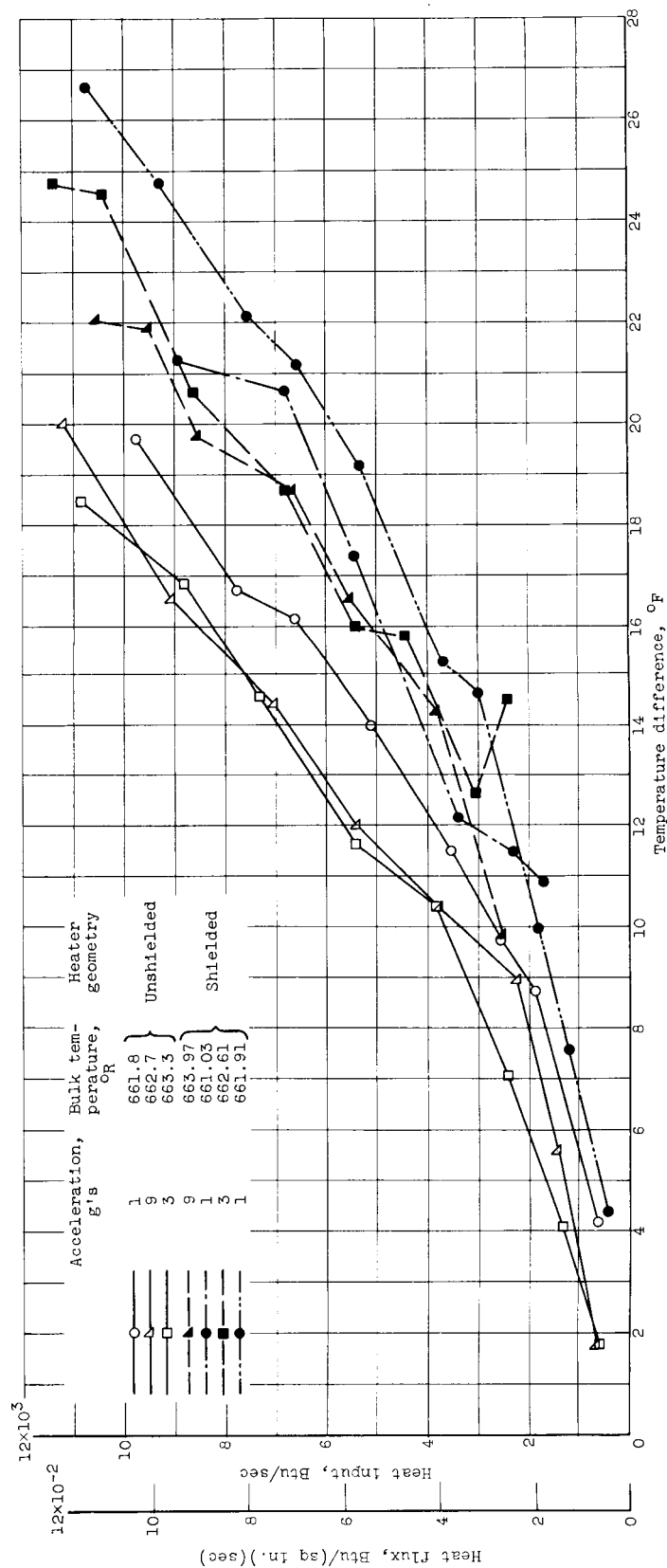


Figure 6. - Influence of shielding geometry on boiling curves (active segment of heater ribbon). Bulk temperature, ~200° F; water, 1 atmosphere.

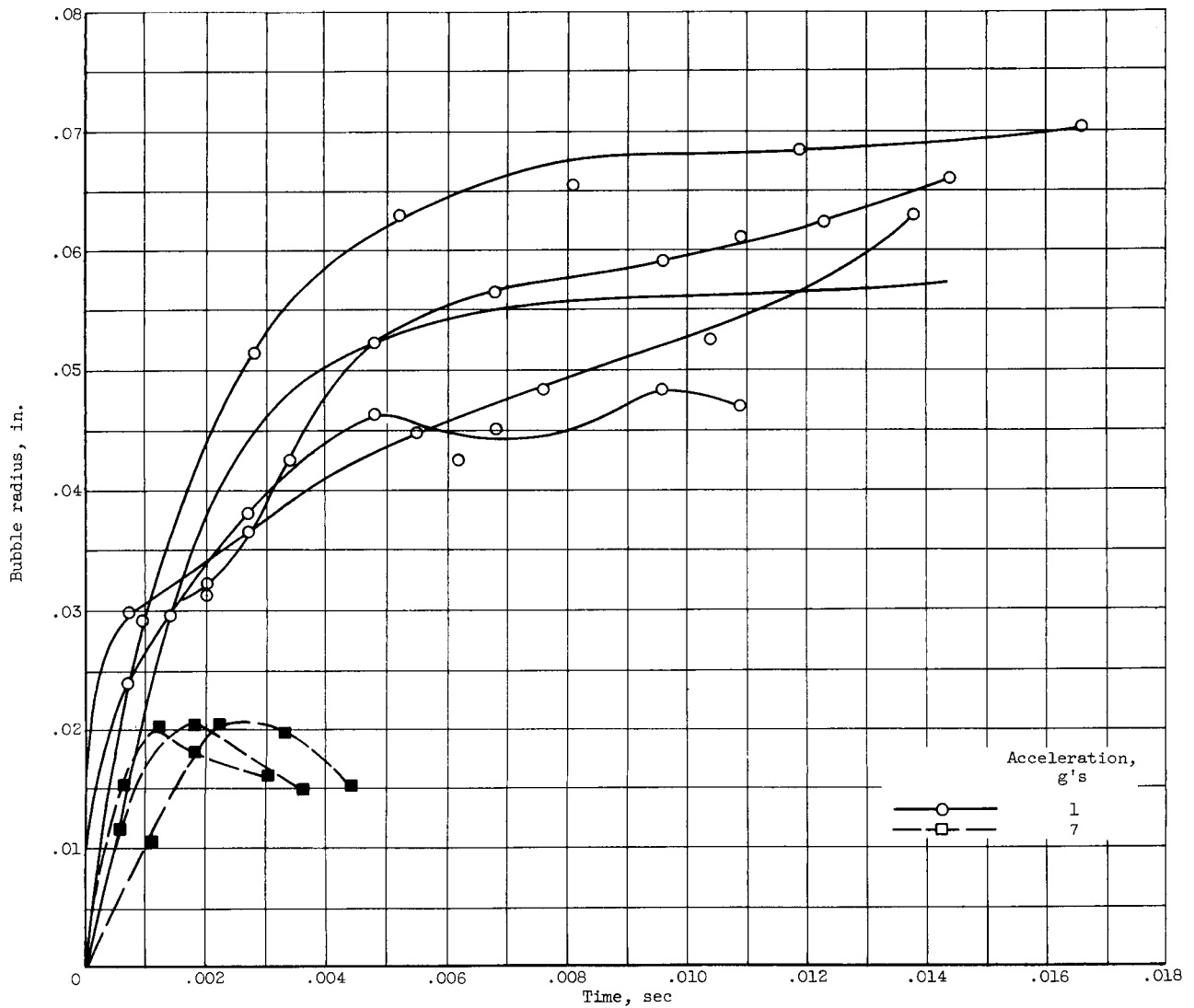


Figure 7. - Effect of acceleration on bubble growth. Bulk temperature,  $\sim 200^{\circ}$  F; water, 1 atmosphere.

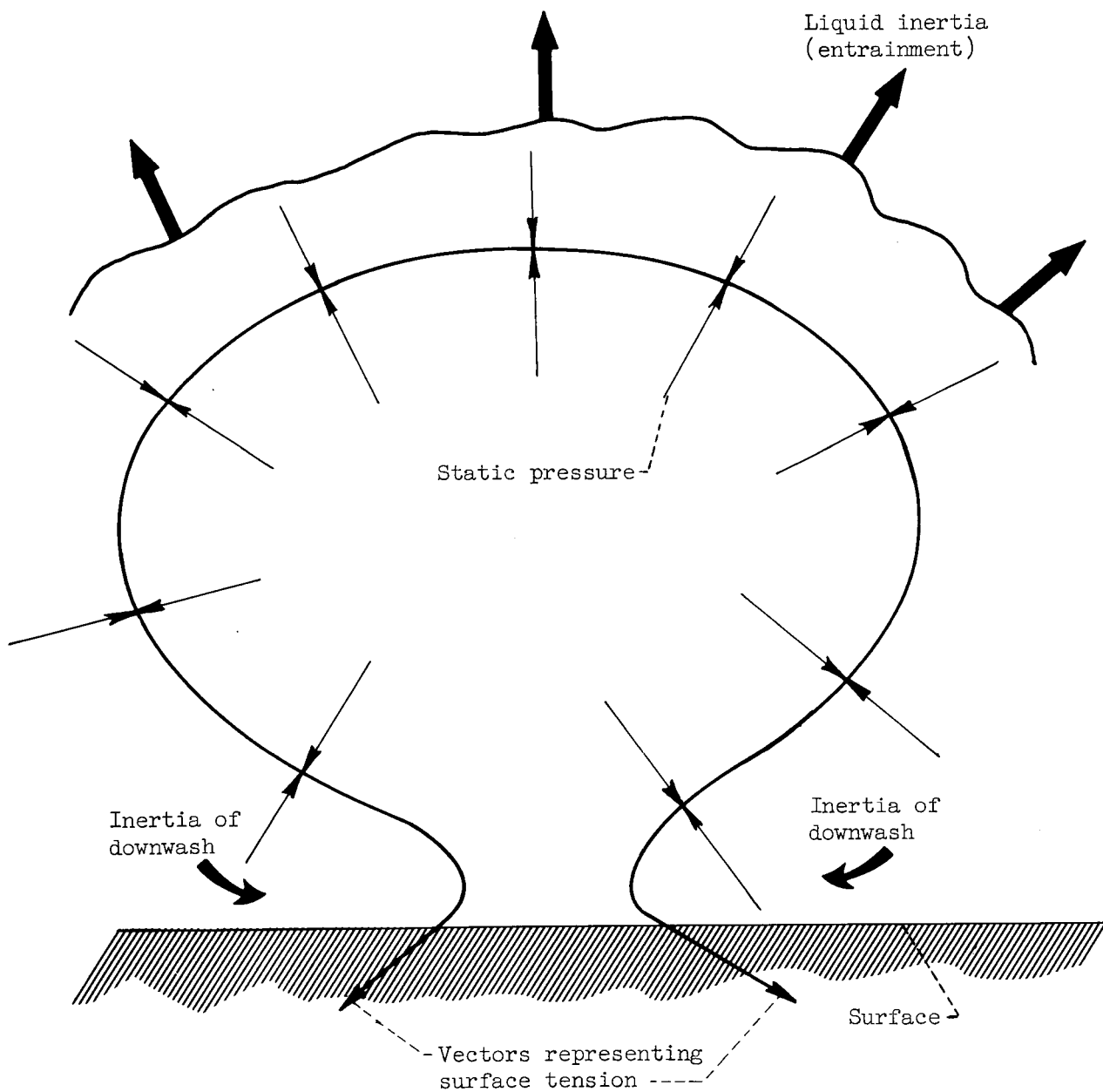


Figure 8. - Schematic of forces acting on growing bubble.

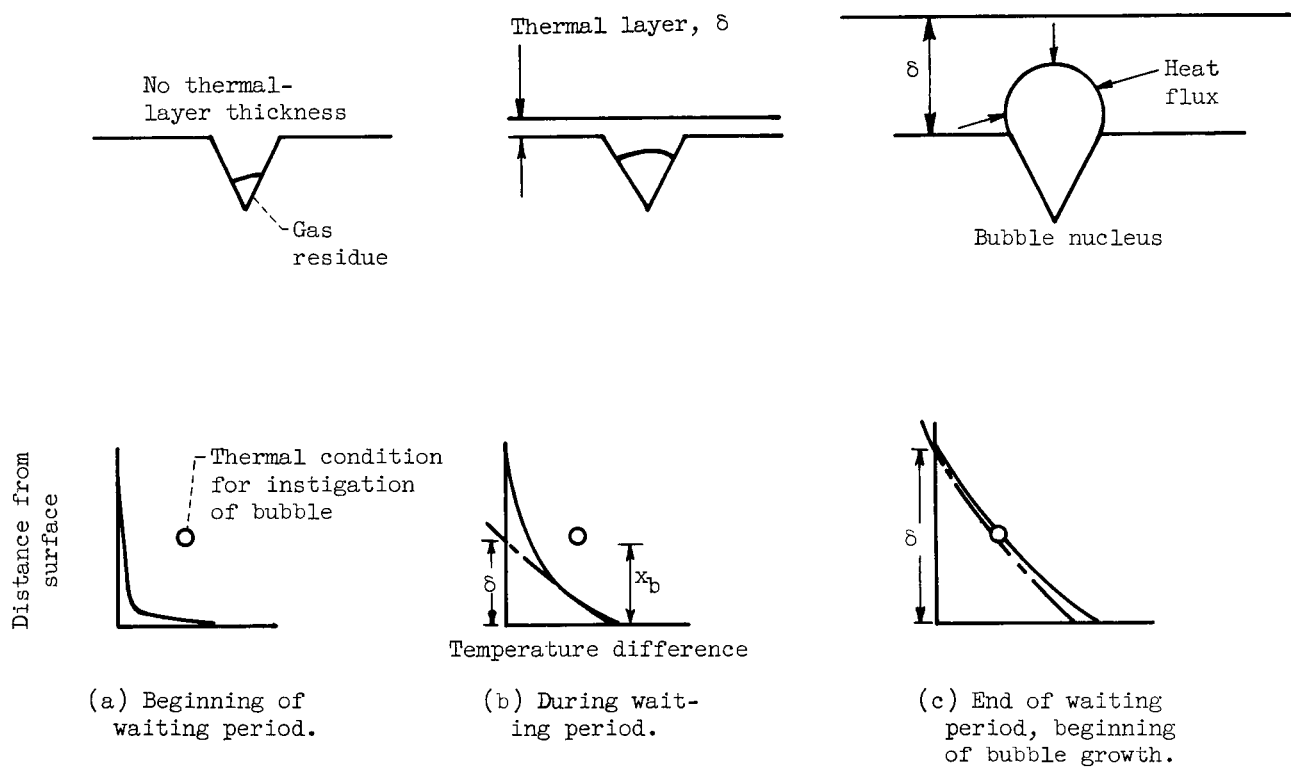


Figure 9. - Schematic of bubble instigation requirements and definition of waiting period.

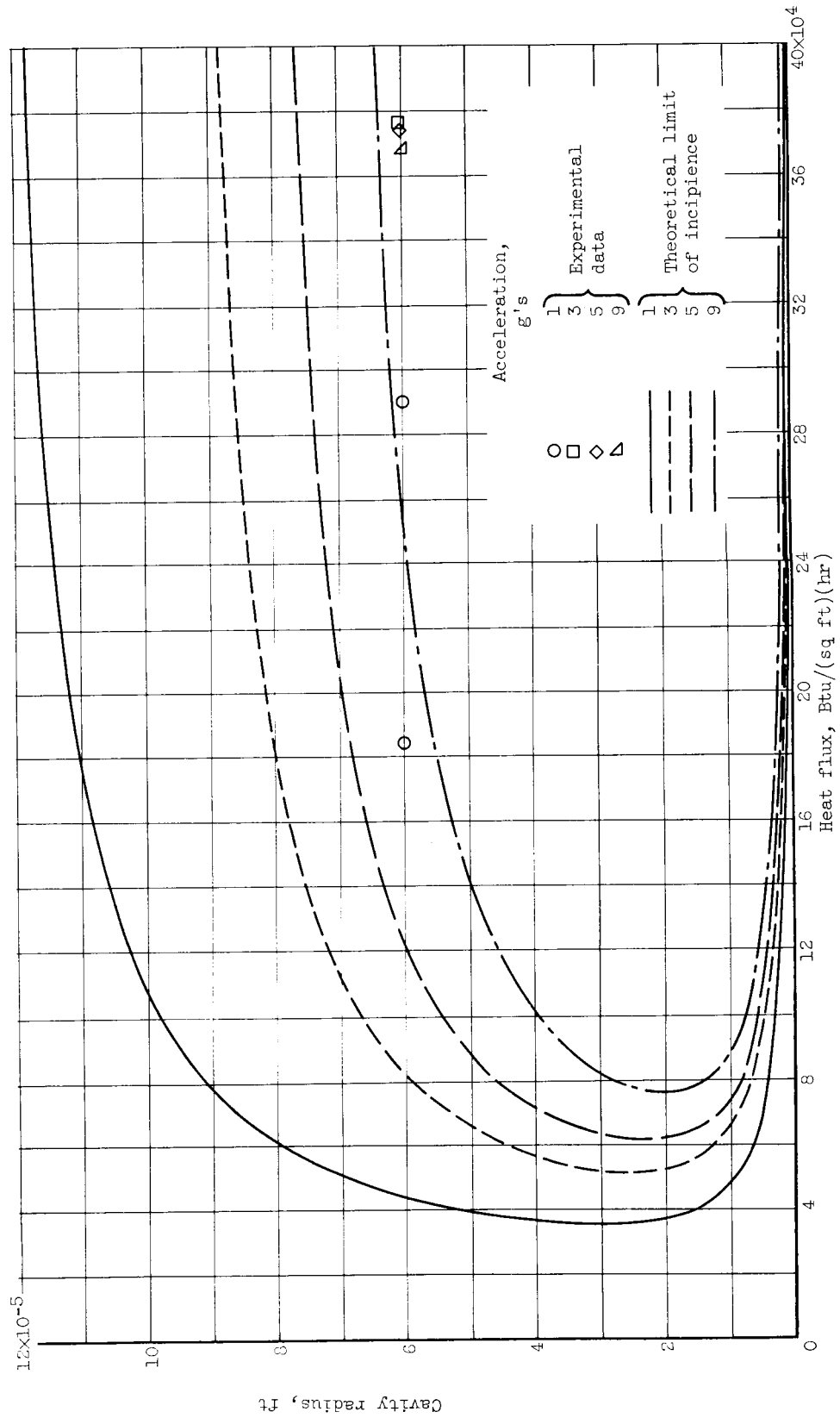


Figure 10. - Comparison of incipient boiling point for various accelerations with theory of reference 7. Bulk temperature, 200° F.

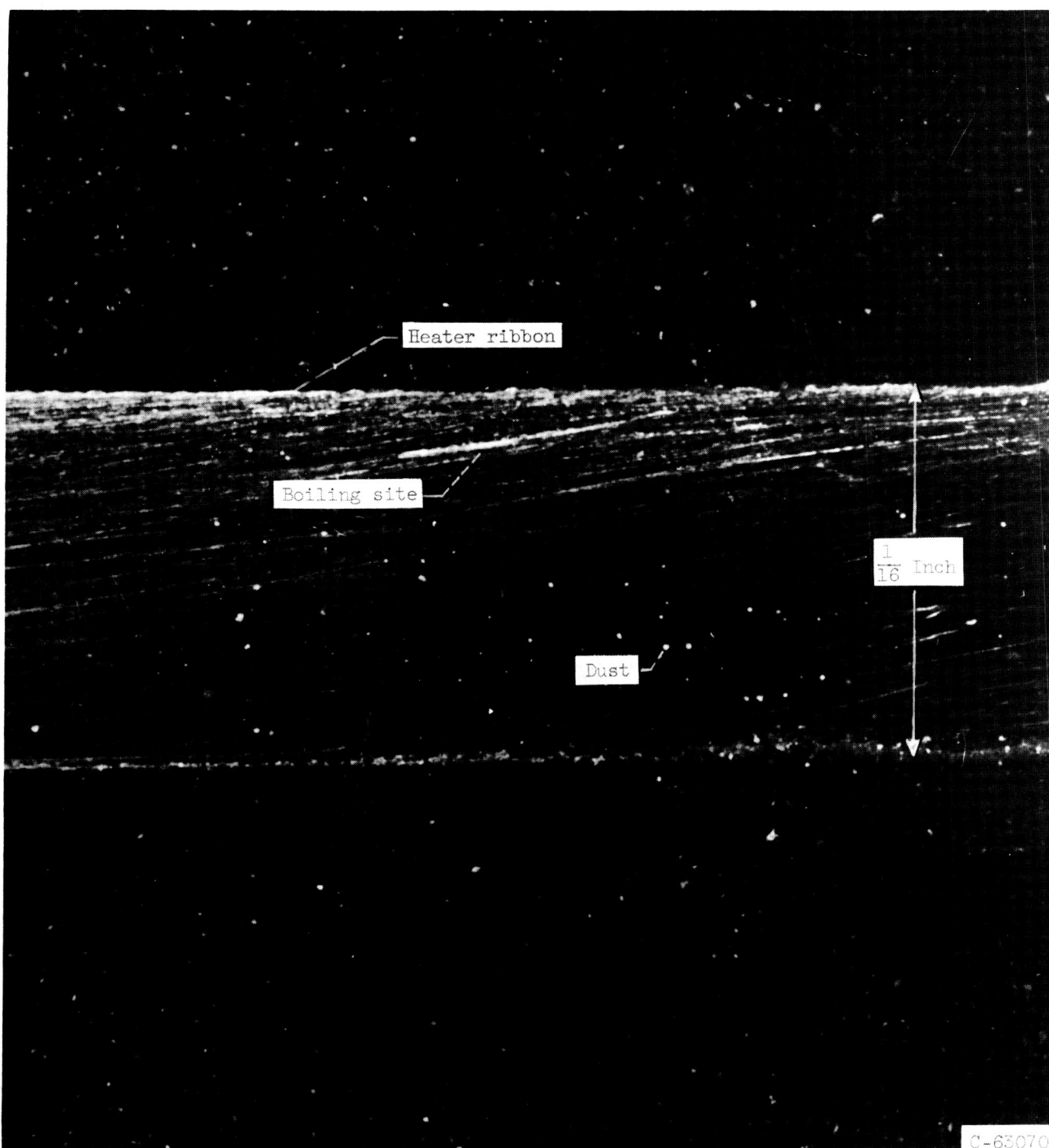


Figure 11. - Active cavity site on heater geometry.

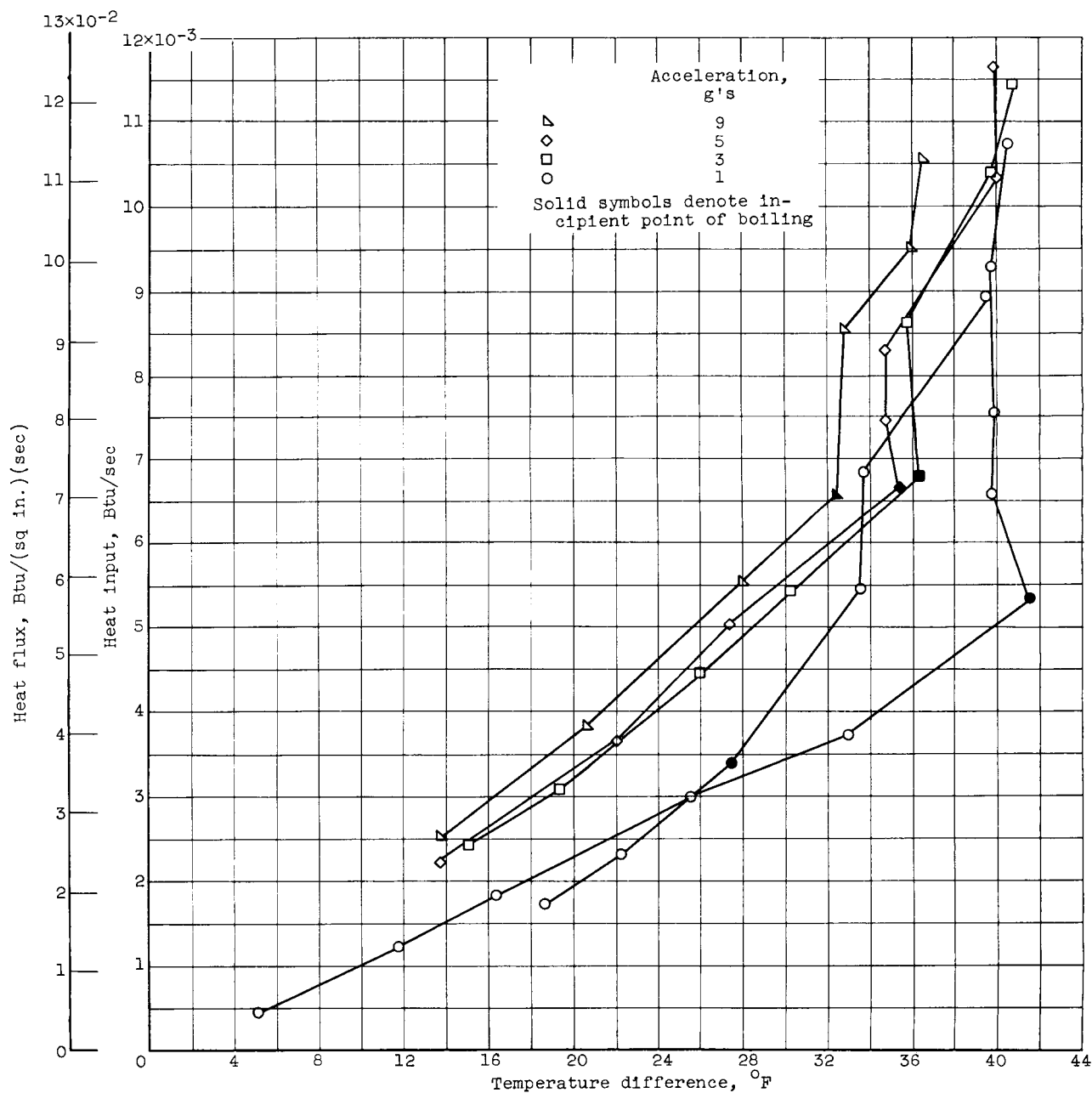


Figure 12. - Pool boiling at isolated site of heater. Water, 1 atmosphere.